Increasing Accuracy in Nonlinear Sliding-Mode Observers without Decreasing Sampling Time Using Frequency Domain Analysis

M. Hajatipour, M. Farrokhi*
Department of Electrical Engineering,
Iran University of Science and Technology, Tehran 16846, IRAN

Abstract: This paper presents a method to improve estimation accuracy of Sliding-Mode Observers (SMOs) using frequency domain analysis. First, the high gain property of the SMO is employed in order to obtain fast convergence of the estimated states. Then, when the system is in the switching condition, signals are decomposed into two parts in the frequency domain: 1) the slow-mode part, which consists of the main signals and 2) the fast-mode part, which consists of the unwanted high-frequency chatterings. In addition, a linear compensator is designed and added in cascade with the observer based on the relay feedback systems theory. In this approach, without reducing the sampling time, the high-gain property is provided for the slow-mode of the observer and at the same time the amplitude of chatterings becomes effectively smaller. Simulation results show good performance of the proposed method as compared to the conventional SMO, when applied to a bioreactor.

Keywords: Sliding-mode observers; Relay-feedback systems; High-gain observers; Switching frequency; Linear compensator

1. Introduction

In practice, a precise model for a real system is often not available due to unknown disturbances and/or uncertain parameters. Sliding-mode Observers (SMOs) are known to be robust against presence of disturbances and/or modeling uncertainties (Picó et al., 2009; Spurgeon, 2008; Veluvolu et al., 2007).

SMOs are known as the high-gain observers, which have appropriate behavior in disturbance rejection (López and Yescas, 2005; Aguilar et al., 2003; Cunha et al., 2009). Vasiljevic and Khalil (2008) have shown that a high-gain observer acts as a differentiator in the limit as the relay gain approaches infinity. In addition, as Ahrens and Khalil (2009) and Pan et al. (2009) have shown, the robustness of SMOs is directly related to the relay gain.

Since the main source of the sliding phenomena is the relay element, some researchers use the relay feedback systems to analyze sliding mode properties (Boiko, 2007; Boiko, 2005; Boiko and Friedman, 2006). Due to the interesting characteristics of relay feedback systems, research in this area is fast developing. A number of analyzing methods for the modeling of relay feedback systems as well as methods for estimating the switching frequencies and the amplitude of oscillations are discussed by Tsypkin (1984) and Atherton (1975).

For the first time, Boiko and Fridman (2006) and Boiko (2009) applied the relay feedback concept to design a linear SMO, where they have used the relay equivalent gain technique in the sliding phase in order to extract the relay equivalent gain. However, no systematic method has been presented to make the relay equivalent gain as high as possible in a linear SMO. Some authors have developed methods to make SMOs robust against disturbances, such as disturbance in the input (Floquet et al., 2007), the measurement noise (Ahrens and Khalil, 2009), and robustness against uncertainties (Spurgeon, 2008; Zheng et al., 2000; Koshkouei and Zinober, 2004). Nevertheless, there is a lack of research on estimation properties in the sliding phase of SMOs. That is, when the sliding surface is reached, state estimation may not have appropriate quality in presence of large uncertainties and disturbances due to insufficient amplitude of the relay equivalent gain.

For the first time, the authors of this paper have used the relay feedback concept in noise effect reduction for nonlinear SMOs (Hajatipour and Farrokhi, 2010). In this work, using a linear compensator with variable structure, the relay equivalent gain in the sliding phase is regulated such that the observer dynamics is less affected by the input noise.

As it will be shown in this paper, in the sliding phase, the relay gain does not affect the relay equivalent gain and the quality of the estimated signals, but rather it improves the robustness of the SMO and the chattering amplitude. In other words, the proposed method improves the estimation accuracy of the SMOs in the presence of uncertainties. This method takes advantage of the high-gain property of SMOs in order to enforce the estimated states to move swiftly to the system states. Therefore, in the first step, the conditions for forcing the observer to go to the sliding-mode phase are satisfied. Next, when the observer is in the sliding condition, signals are decomposed into two parts: the slow-mode part and the fast-mode part. The slow-mode part contains important information about the estimated signals while the fast mode part contains the oscillation or chattering signals. For every mode, the corresponding design for the appropriate operation of the observer will be considered. It will be shown that the amplitude and frequency of oscillations have direct effects on the dynamics and stability of the fast and slow-mode parts of the states estimation when the observer is operating in the sliding phase. Next, the relationship between the sampling time and the quality of estimation in the SMO is analyzed. In addition, in order to obtain fast convergence and better estimated signals in the sliding phase, a linear compensator with special frequency domain properties is connected in series with the SMO. This compensator provides a high equivalent gain for the relay, which improves the quality of the state estimation against uncertainties without any need to reduce the sampling time.

The main features of the proposed method can be summarized as follows:

- Frequency regulation of the nonlinear SMO without any need for linearization.
- Presenting a relationship between the switching frequency, stability, and performance of the SMO.
- Presenting a relationship between the sampling time and the estimation accuracy of the SMO in presence of uncertainties.
- Providing high-gain property to the sliding phase of the SMO and consequently obtaining more accuracy of the estimated signals without any need to reduce the sampling time.

Simulation results show good performance of the proposed method as compared to the conventional SMO when it is applied to a bioreactor.

This paper is organized in six sections. Section 2 gives the problem statement, preliminary definitions and assumptions. Sections 3 and 4 provide the design procedure of the proposed method. Section 5 shows illustrative example followed by conclusions in Section 6.

Notations: Throughout this paper, $\lambda_{\max}(\mathbf{A})$ denotes the maximum eigenvalue of matrix **A**, $\|\mathbf{A}\|$ denotes the 2-norm of it and Re is the real part of a complex number.

General Definitions: A function Υ is said to belong to the class-$\mathcal{K}$ ($\Upsilon \in \mathcal{K}$) if it is continuous, zero at zero, and strictly increasing. A function $\Pi : \mathbb{R}_+ \times \mathbb{R}_+ \to \mathbb{R}_+$ is said to belong to the class-$\mathcal{KL}$ ($\Pi \in \mathcal{KL}$) if it satisfies: (i) for $t \geq 0$, $\Pi(\cdot, t)$ is non-decreasing and $\lim_{s \to 0^+} \Pi(s, t) = 0$, and (ii) for $s \geq 0$, $\Pi(s, \cdot)$ is non-increasing and $\lim_{t \to \infty} \Pi(s, t) = 0$.

2. Problem statement

Consider the following class of systems:

$$\begin{aligned} \dot{\mathbf{x}} &= \mathbf{A}\mathbf{x} + \mathbf{f}(\mathbf{x}, \mathbf{u}) + \mathbf{E}\psi(\mathbf{x}, \mathbf{u}) \\ y &= \mathbf{C}\mathbf{x} \end{aligned} \tag{1}$$

where $\mathbf{x} \in \Re^n$ is the vector of unknown state variables, $\mathbf{u} \in \Re^m$ is the input signal, $y \in \Re$ is the measured output, $\mathbf{f} : \Re^n \times \Re^m \to \Re^n$ is a nonlinear smooth function, and $\mathbf{E} \in \Re^{n \times 1}$ and $\psi : \Re^n \times \Re^m \to \Re$ are the modeling uncertainties and disturbances, respectively.

Assumption 1: The uncertainty function ψ is assumed to be bounded. That is, $|\psi(\mathbf{x}, \mathbf{u})| \leq \bar{\psi}$, where $\bar{\psi}$ is the known upper bound.

Assumption 2: The nonlinear function $\mathbf{f}(\mathbf{x}, \mathbf{u})$ is Lipschitz with respect to $\mathbf{x}$ and uniformly for $\mathbf{u} \in \mathfrak{A}$, where $\mathfrak{A}$ is an admissible control set. That is, there exists a constant $\gamma > 0$ such that

$$\left\| \mathbf{f}(\mathbf{x}, \mathbf{u}) - \mathbf{f}(\hat{\mathbf{x}}, \mathbf{u}) \right\| \leq \gamma \left\| \mathbf{x} - \hat{\mathbf{x}} \right\|. \tag{2}$$

Figure 1 presents the structure of the proposed observer, which has the following form:

$$G_{\text{OBS}} := \begin{cases} \dot{\hat{\mathbf{x}}} = \mathbf{A}\hat{\mathbf{x}} + \mathbf{f}(\hat{\mathbf{x}}, \mathbf{u}) + \mathbf{L}(y - \hat{y}) + \mathbf{E}\,\bar{y} \\ \hat{y} = \mathbf{C}\hat{\mathbf{x}} \end{cases} \tag{3}$$

where $\hat{\mathbf{x}}$ denotes the estimated state vector and $\mathbf{L}$ is the observer gain matrix. In Figure 1, L.P.F denotes a linear low pass filter that will be designed later on. Moreover, $\bar{y}$ is the output of the following linear stable SISO system, which has the relative degree of zero:

$$H := \begin{cases} \dot{\xi} = \mathbf{M}\xi + \mathbf{N}\bar{u} \\ \bar{y} = \mathbf{S}\xi + R\bar{u} \end{cases}, \tag{4}$$

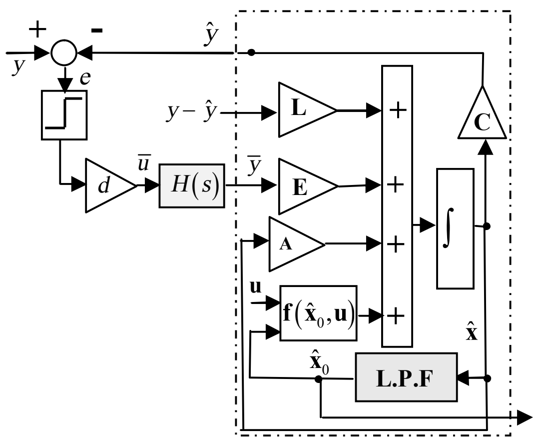

Figure 1. Structure of the Proposed observer

where $\mathbf{M}$, $\mathbf{N}$ and $\mathbf{S}$ are constant matrices with appropriate dimensions, R a positive scalar and $\xi \in \Re^q$ and $\bar{u} \in \Re$ are the state vector and the input signal, respectively.

Since the eigenvalues of $H(s)$ are all negative, from the theory of passivity (Slotine and Li, 1991)

$$\mathrm{Re}\{H(j\Omega)\} > 0 \quad \forall \Omega \geq 0,$$

where $\mathrm{Re}\{H(j\Omega)|_{\Omega=0}\} = -\mathbf{SM}^{-1}\mathbf{N}$. Hence,

$$\mathbf{SM}^{-1}\mathbf{N} = -\kappa, \tag{5}$$

where κ is a positive constant.

Assumption 3: System (1) is observable. Moreover, an estimation gain $\mathbf{L}$ can be designed such that ($\mathbf{A}$–$\mathbf{LC}$) is stable.

Next, by defining $e := y - \hat{y}$, it gives

$$\bar{u} = d\,\mathrm{sgn}(e), \tag{6}$$

where $d \geq 0$ is the relay gain.

Since system (4) has stable poles and zeroes, it is input-to-state stable. That is

$$\|\xi(t)\| \leq \Pi\left(\|\xi(t_0)\|, t - t_0\right) + \Upsilon\left(\sup_{t_0 \leq \tau \leq t} \|\bar{u}(\tau)\|\right) \quad \forall t \geq t_0 \geq 0, \tag{7}$$

where Π and Υ are functions belong to the classes of $\mathcal{KL}$ and $\mathcal{K}$, respectively (Khalil, 1996). Since $\xi(t_0)$ and $\|\bar{u}(\tau)\|$ are bounded, then, according to (7), $\|\xi(t)\|$ is bounded too. That is $\|\xi(t)\| \leq \chi_1$. Hence, based on (4), the following inequality can be obtained:

$$\begin{aligned} \|\dot{\xi}\| &\leq \|\mathbf{M}\|\|\xi\| + \|\mathbf{N}\|\|\bar{u}\| \leq \|\mathbf{M}\|\chi_1 + \|\mathbf{N}\|d \\ &\leq \chi_2 \end{aligned} \tag{8}$$

Defining the state estimation error as $\boldsymbol{\sigma} := \mathbf{x} - \hat{\mathbf{x}}$, the error dynamics become

$$\dot{\boldsymbol{\sigma}} = \bar{\mathbf{A}}\boldsymbol{\sigma} + \left(\mathbf{f}(\mathbf{x},\mathbf{u}) - \mathbf{f}(\hat{\mathbf{x}},\mathbf{u})\right) + \mathbf{E}\left(\psi(\mathbf{x},\mathbf{u}) - \bar{y}\right), \tag{9}$$

where $\bar{\mathbf{A}} = \mathbf{A} - \mathbf{LC}$. Augmenting (4) and (9) gives a new set of state variables as

$$\begin{bmatrix} \dot{\boldsymbol{\sigma}} \\ \dot{\xi} \end{bmatrix} = \begin{bmatrix} \bar{\mathbf{A}} & -\mathbf{ES} \\ 0 & \mathbf{M} \end{bmatrix} \begin{bmatrix} \boldsymbol{\sigma} \\ \xi \end{bmatrix} + \begin{bmatrix} \left(\mathbf{f}(\mathbf{x},\mathbf{u}) - \mathbf{f}(\hat{\mathbf{x}},\mathbf{u})\right) + \mathbf{E}\psi(\mathbf{x},\mathbf{u}) \\ 0 \end{bmatrix} + \begin{bmatrix} -\mathbf{E}R \\ \mathbf{N} \end{bmatrix} \bar{u}, \tag{10}$$

The proposed observer is designed for two different phases: 1) the reaching phase and 2) the sliding phase. In the reaching phase, the observer is a high-gain observer. That is, the high-gain property of the relay (*d*) guarantees fast convergence of the estimation errors and forces the observer into the sliding phase. Moreover, this high gain can provide better disturbance rejection. In the sliding phase, on the other hand, a novel approach will be proposed where the signals are decomposed into the slow- and fast-mode parts, each part requiring a different design. Next, based on the obtained results, the relationship between the sampling time and the accuracy of estimation of the SMO will be analyzed. Then, an approach will be proposed that improves performance of the SMO in the presence of uncertainties and disturbances without any need to reduce the sampling time. The proposed method takes advantage of a linear compensator cascaded with the SMO that increases the relay equivalent gain. In fact, in the sliding phase, this compensator provides swift convergence of the slow-mode part of the estimation error to zero. Moreover, since the compensator acts as a low-pass filter, the amplitude of oscillations is effectively decreased.

In the rest of this paper, the objective is to design *d*, $H(s)$ and **L** to achieve the aforementioned goals.

Definition 1: Due to the presence of a discontinues term in the relay, signals in the sliding phase can be decomposed into two parts: 1) the fast-mode part associated with the periodical motion across the sliding surface and 2) the slow-mode part associated with the motion along the sliding surface. Let us define $\Omega \leq \Omega_b$ as the low-frequency domain and $\Omega > \Omega_b$ as the high-frequency domain, where Ω_b is defined as the bandwidth frequency of the slow-mode part of the observer in the sliding phase. Therefore, every signal in the system and in the observer can be decomposed into two parts: 1) the slow-mode part and 2) the fast-mode part; i.e.

$$\mathbf{x} = \mathbf{x}_0 + \mathbf{x}_s \,,\ e(t) = e_0(t) + e_s(t) \,,\ \boldsymbol{\sigma} = \boldsymbol{\sigma}_0 + \boldsymbol{\sigma}_s \,,\ y = y_0 + y_s \,,\ \hat{y} = \hat{y}_0 + \hat{y}_s \,,\ \bar{y} = \bar{y}_0 + \bar{y}_s \,,$$

where subscripts “0” and “s” indicate the slow- and the fast-mode parts of the corresponding signal, respectively. This separating idea has been used before for linear systems by Boiko (2008) and Boiko et al. (2009).

Remark 1: As it will be considered later, since the frequency of the fast-mode part can be designed high enough and far from the bandwidth of the slow-mode part of the observer (Ω_b), then by passing signals through a low-pass filter with a bandwidth greater than Ω_b but smaller than the switching frequency (Ω_s), which is high enough, the high-frequency mode can be removed from the estimated states. This idea was proposed before by other researchers such as (Haskara et al., 1998). Hence, the main system just observes the slow-mode part of the estimated state variables that has frequency in the domain of $\Omega \leq \Omega_b$. Without any loss of generality, it can be assumed that the frequency of the main part of the system signals (i.e. the part that need to be estimated) is in the domain of $\Omega \leq \Omega_b$. The other part of the system signals, which is in the domain of $\Omega > \Omega_b$, is not important as compared to the observer high-frequency mode and hence, can be eliminated. Therefore, the high-frequency parts of the main system signals, i.e. $y_s(t)$ and $\mathbf{x}_s(t)$, can be eliminated. That is, it can be assumed that $\mathbf{x}_s = 0$ and $y_s(t) = 0$.

In the next section, the observer design for the reaching phase as well as the sliding phase will be given.

3. Observer Design

In this section, the observer design will be presented for two different phases. First, in the reaching phase, conditions for forcing the estimated states to move quickly to the sliding phase will be defined. Due to the high amplitude of the relay gain (*d*), this mode acts as a high-gain observer. Next, in the sliding phase, the observer dynamics for the slow- and the fast-mode parts are derived. In addition, the properties of every mode will be analyzed. Moreover, in the sliding phase, the estimation quality can be improved by the proper design of *H*(*s*).

3.1. Reaching phase

In this subsection, it will be shown that proper selection of the relay gain (*d*), guarantees convergence of the error dynamics to the sliding surface in finite time and that the sliding condition occurs.

Remark 2. Before the sliding phase occurs, all signals have only their slow-mode part. Hence, the low-pass filter in Figure 1 does not affect the observer dynamics before the sliding phase occurs.

Let us define $\mathbf{C}\boldsymbol{\sigma} := e = y - \hat{y} = 0$ as the sliding surface. It is well known that the sliding surface and its derivative must satisfy $e = \dot{e} = 0$ in the sliding phase. The condition for the existence of a sliding phase is (Utkin, 1992):

$$e\dot{e} < 0 \quad \forall e \neq 0 \text{ and } \forall t \geq t_0 . \tag{11}$$

Then, it is said that the surface $e = 0$ is an attracting surface and the sliding condition occurs.

Assumption 4: The positive definite matrix $\mathbf{P}_1 = \mathbf{P}_1^T$ and matrix $\mathbf{L}$ satisfy the following equation:

$$(\mathbf{A} - \mathbf{LC})^T \mathbf{P}_1 + \mathbf{P}_1^T (\mathbf{A} - \mathbf{LC}) = -\mathbf{Q}_1 , \tag{12}$$

where $\mathbf{A}$ is Hurwitz and $\mathbf{Q}_1$ is positive definite.

Since in the reaching phase $\bar{u}(t)$ in (4) is fixed, then, based on the theory of linear systems (Kailath, 1980) $\bar{y}(t)$ can be written as

$$\bar{y}(t) = \mathbf{S}e^{\mathbf{M}t}\xi(t_0) + \left[\mathbf{S}\mathbf{M}^{-1}e^{\mathbf{M}t}\mathbf{N} - \mathbf{S}\mathbf{M}^{-1}\mathbf{N}\right]\bar{u}(t) + R\ \bar{u}(t) = \boldsymbol{\Xi}(t)\ \bar{u}(t) , \tag{13}$$

where R and $-\mathbf{S}\mathbf{M}^{-1}\mathbf{N}$ are positive scalars defined in (4) and (5), respectively. For small values of $\xi(t_0)$, one can conclude that $0 < \Xi_L \leq \Xi(t) \leq \bar{\Xi}$, where Ξ_L and $\bar{\Xi}$ are the lower and upper bounds of function $\Xi(t)$, respectively (see Appendix A for more details).

Assumption 5: Matrix $\mathbf{P}_1$ in (12) can be defined such that $\mathbf{P}_1\mathbf{E} = \mathbf{C}^T + \bar{\mathbf{C}}$, where $\bar{\mathbf{C}} = \mathbf{W}\mathbf{P}_1\mathbf{E}$, in which $\mathbf{W}$ is an appropriate matrix.

Lemma 1: Consider Assumptions 1--5, Remark 1, and the error dynamics (10). By Selecting the sliding gain d as follows, it guarantees that the sliding surface will be reached:

$$d \geq \bar{d} \qquad \forall \boldsymbol{\sigma} \in \Re^n , \tag{14}$$

where

$$\bar{d} = \|\mathbf{C}\|\,\|\boldsymbol{\sigma}\|\left(\|\mathbf{A} - \mathbf{LC}\| + \gamma\right) + \|\mathbf{C}\|\|\mathbf{E}\|\bar{\psi}/(\mathbf{CE}\Xi_L),$$

in which γ, Ξ_L and $\bar{\psi}$ are the same as defined before.

Proof: Let us define the following Lyapunov function:

$$V_1 = \frac{1}{2}e^2 . \tag{15}$$

According to (9) the time derivative of V_1 is

$$\begin{aligned} \dot{V}_1 &= e\dot{e} \\ &= e\mathbf{C}\left[\left((\mathbf{A} - \mathbf{LC})\boldsymbol{\sigma} + \mathrm{f}(\mathbf{x},\mathbf{u}) - \mathrm{f}(\hat{\mathbf{x}},\mathbf{u}) + \mathbf{E}\psi(\mathbf{x},\mathbf{u})\right) - \mathbf{E}\bar{y}\right]. \end{aligned} \tag{16}$$

Then from (13) and (6) we have

$$\begin{aligned} \dot{V}_1 &\leq \|e\|\left[\|\mathbf{C}\|\,\|\boldsymbol{\sigma}\|\left(\|\mathbf{A} - \mathbf{LC}\| + \gamma\right) + \|\mathbf{C}\|\|\mathbf{E}\|\bar{\psi}\right] - \mathbf{CE}\boldsymbol{\Xi}(t)\,d\,\|e\| \\ &= \|e\|\left[\|\mathbf{C}\|\,\|\boldsymbol{\sigma}\|\left(\|\mathbf{A} - \mathbf{LC}\| + \gamma\right) + \|\mathbf{C}\|\|\mathbf{E}\|\bar{\psi} - \mathbf{CE}\boldsymbol{\Xi}(t)\,d\right]. \end{aligned} \tag{17}$$

Next, the condition for $\dot{V}_1 \leq 0$ is

$$d \geq \|\mathbf{C}\|\,\|\boldsymbol{\sigma}\|\left(\|\mathbf{A} - \mathbf{LC}\| + \gamma\right) + \|\mathbf{C}\|\|\mathbf{E}\|\bar{\psi}/\left(\mathbf{CE}\boldsymbol{\Xi}(t)\right). \tag{18}$$

Now, let us define

$$\bar{d} := \|\mathbf{C}\| \|\boldsymbol{\sigma}\| \left(\|\mathbf{A} - \mathbf{LC}\| + \gamma \right) + \|\mathbf{C}\| \|\mathbf{E}\| \bar{\psi} / \left(\mathbf{CE}\Xi_L \right). \tag{19}$$

Hence, selecting $d \geq \bar{d}$ guarantees $\dot{V}_1 < 0$. Therefore, condition (14) ensures that the sliding surface $e = \mathbf{C}\boldsymbol{\sigma} = 0$ can be reached and that the sliding condition occurs. □

3.2. Sliding phase

It is well known that the describing function (DF) of the relay element in the sliding phase can be obtained based on its input amplitude and its gain (*d*) (Åström and Wittenmark, 1995). Next, the DF of the relay element will be defined.

3.2.1 Relay model in the sliding phase

The relay element was defined in (6), where *d* is the relay gain. As it will be shown latter, the fast-mode dynamics of the observer is a linear system. It is well known that in linear relay-feedback systems, the high-frequency part of *e*(*t*) (i.e., the input signal to the relay element) can be presented as (Åström and Wittenmark, 1995)

$$e_s(t) = a \sin(\Omega_s t), \tag{20}$$

where a and Ω_s are the amplitude and frequency of the limit cycle (or oscillations), respectively. Using the Fourier transform, $\bar{u}(t)$ can be presented as (Åström and Wittenmark, 1995)

$$\bar{u}(t) = K_n e_0(t) + K_s a \sin(\Omega_s t) + K_{s1} a \sin(2\Omega_s t) + \cdots, \tag{21}$$

where K_n, K_s, K_{s1}, … can be determined using the Fourier transform. Hence, $\bar{u}(t)$ can be written as

$$\bar{u}(t) = K_n e_0(t) + K_s e_s(t) + N_\varepsilon(\cdot), \tag{22}$$

where $N_\varepsilon(\cdot)$ is the modeling error. Since Ω_s can be selected high enough in the design procedure and because most systems in engineering applications act as a low pass filter and in view of the fact that $N_\varepsilon(\cdot)$ contains signals with frequencies larger than Ω_s, the effect of $N_\varepsilon(\cdot)$ in the estimated states is very trivial and can be ignored. Nevertheless, it will be considered in the analysis that follows.

Assumption 6: $N_\varepsilon(\cdot)$ is unknown but bounded and its norm can be represented as

$$\|N_\varepsilon(\cdot)\| < \beta_1 \|\boldsymbol{\sigma}_0\| + \beta_2, \tag{23}$$

where $\boldsymbol{\sigma}_0$ is the low-frequency part of the error signal $\boldsymbol{\sigma}$ and β_1 and β_2 are positive constants.

Since $e_0(t) = \mathbf{C}\boldsymbol{\sigma}_0(t)$ and $e_s(t) = \mathbf{C}\boldsymbol{\sigma}_s(t)$, (22) can be written as

$$\bar{u}(t) = K_n \mathbf{C}\boldsymbol{\sigma}_0(t) + K_s \mathbf{C}\boldsymbol{\sigma}_s(t) + N_\varepsilon(\cdot), \tag{24}$$

where K_n and K_s can be computed as (Boiko, 2005; Åström and Wittenmark, 1995)

$$K_n = \left. \frac{\partial \bar{u}_0}{\partial \sigma_y} \right|_{\bar{u}_0 = 0} = \frac{2d}{\pi a}, \tag{25}$$

$$K_s = \frac{4d}{\pi a}. \tag{26}$$

Hence, the relay element passes the slow-mode part of signals with the gain K_n and the fast-mode part of signals with the gain K_s; i.e.

$$\bar{u}_s(t) = K_s \mathbf{C}\boldsymbol{\sigma}_s(t), \tag{27}$$

$$\bar{u}_0(t) = K_n \mathbf{C}\boldsymbol{\sigma}_0(t). \tag{28}$$

3.2.2 Observer structure in sliding phase

In order to derive the main results, first by considering two modes of signals in the sliding phase (based on Definition 1), (10) can be rewritten as

$$\begin{bmatrix}\dot{\boldsymbol{\sigma}}_0+\dot{\boldsymbol{\sigma}}_s\\ \dot{\xi}_0+\dot{\xi}_s\end{bmatrix}=\begin{bmatrix}\bar{\mathbf{A}} & -\mathbf{ES}\\ 0 & \mathbf{M}\end{bmatrix}\begin{bmatrix}\boldsymbol{\sigma}_0+\boldsymbol{\sigma}_s\\ \xi_0+\xi_s\end{bmatrix}+\begin{bmatrix}\left(\mathbf{f}(\mathbf{x}_0+\mathbf{x}_s,\mathbf{u})-\mathbf{f}(\hat{\mathbf{x}}_0+\hat{\mathbf{x}}_s,\mathbf{u})\right)+\mathbf{E}\psi(\mathbf{x}_0+\mathbf{x}_s,\mathbf{u})\\ 0\end{bmatrix}+\begin{bmatrix}-\mathbf{E}R\\ \mathbf{N}\end{bmatrix}\bar{u}\,. \tag{29}$$

Note that based on Remark 1 and as Figure 1 shows, the high-frequency modes of the system signals (i.e. $\mathbf{x}_s$) can be eliminated from (29) using a low pass filter. In addition, in the observer structure, the high-frequency mode of the estimated signals (i.e. $\hat{\mathbf{x}}_s$) is filtered if it is just used as the states of a nonlinear function such as $\mathbf{f}(\cdot)$ in (1). This task, as it will be shown shortly, changes the high-frequency mode of the proposed observer into a linear system. Consequently, this part of the observer obeys theories of linear relay-feedback systems.

Using (24), (29) can be written as

$$\begin{bmatrix}\dot{\boldsymbol{\sigma}}_0+\dot{\boldsymbol{\sigma}}_s\\ \dot{\xi}_0+\dot{\xi}_s\end{bmatrix}=\begin{bmatrix}\bar{\mathbf{A}} & -\mathbf{ES}\\ 0 & \mathbf{M}\end{bmatrix}\begin{bmatrix}\boldsymbol{\sigma}_0+\boldsymbol{\sigma}_s\\ \xi_0+\xi_s\end{bmatrix}+\begin{bmatrix}\mathbf{f}(\mathbf{x}_0,\mathbf{u})-\mathbf{f}(\hat{\mathbf{x}}_0,\mathbf{u})+\mathbf{E}\psi(\mathbf{x}_0,\mathbf{u})\\ 0\end{bmatrix}+\begin{bmatrix}-\mathbf{E}R\\ \mathbf{N}\end{bmatrix}\left(K_n\mathbf{C}\boldsymbol{\sigma}_0(t)+K_s\mathbf{C}\boldsymbol{\sigma}_s(t)+N_\varepsilon(\cdot)\right). \tag{30}$$

Hence, the estimation error dynamics of the observer can be decomposed into the slow- and fast-mode parts, respectively, as

$$G_{\mathrm{SM}}:\begin{bmatrix}\dot{\boldsymbol{\sigma}}_0\\ \dot{\xi}_0\end{bmatrix}=\begin{bmatrix}\bar{\mathbf{A}} & -\mathbf{ES}\\ 0 & \mathbf{M}\end{bmatrix}\begin{bmatrix}\boldsymbol{\sigma}_0\\ \xi_0\end{bmatrix}+\begin{bmatrix}\mathbf{f}(\mathbf{x}_0,\mathbf{u})-\mathbf{f}(\hat{\mathbf{x}}_0,\mathbf{u})+\mathbf{E}\psi(\mathbf{x}_0,\mathbf{u})\\ 0\end{bmatrix}+\begin{bmatrix}-\mathbf{E}R\\ \mathbf{N}\end{bmatrix}\left(K_n\mathbf{C}\boldsymbol{\sigma}_0(t)+N_\varepsilon(\cdot)\right) \tag{31}$$

$$G_{\mathrm{FM}}:\begin{bmatrix}\dot{\boldsymbol{\sigma}}_s\\ \dot{\xi}_s\end{bmatrix}=\begin{bmatrix}\bar{\mathbf{A}} & -\mathbf{ES}\\ 0 & \mathbf{M}\end{bmatrix}\begin{bmatrix}\boldsymbol{\sigma}_s\\ \xi_s\end{bmatrix}+\begin{bmatrix}-\mathbf{E}R\\ \mathbf{N}\end{bmatrix}\left(K_s\mathbf{C}\boldsymbol{\sigma}_s\right), \tag{32}$$

where $\dot{\boldsymbol{\sigma}}_s$ and $\dot{\boldsymbol{\sigma}}_0$ are the observer error dynamics associated with the slow- and fast mode parts, respectively. These two dynamics need to be designed separately. For the slow-mode part, as it will be shown in Theorem 1, K_n must be defined such that $\boldsymbol{\sigma}_0$ becomes very small as $t\to\infty$. On the other hand, for the fast-mode part, $\mathrm{H}(j\Omega)$ and $\mathbf{L}$ must be designed to provide proper values for K_n. In addition, the oscillation frequency must be large enough such that it can be removed by a low pass filter.

3.2.2.1. Slow-mode dynamics of observer in sliding phase

Lemma 1 guarantees convergence of the error dynamics to the sliding surface, which in turn ensures occurrence of the sliding phase. Then, in the sliding phase, as (31) and (32) show, the observer structure consists of two parts.

The following theorem shows the condition to obtain small estimation errors in the presence of uncertainties.

Theorem 1: Consider the slow-mode part of the observation error (31) and Assumptions 1--6. Then, the error dynamics for the slow-mode part (i.e. $\boldsymbol{\sigma}_0$) is uniformly ultimately bounded. Moreover, this bound can be made small enough.

Proof: Consider the following Lyapunov function:

$$V_2=\frac{1}{2}\boldsymbol{\sigma}_0^{\,T}\mathbf{P}_1\boldsymbol{\sigma}_0\,, \tag{33}$$

where $\mathbf{P}_1$ is the same as defined in Assumption 4. Considering (31), the time derivative of (33) is

$$\dot{V}_2 = -\boldsymbol{\sigma}_0{}^T\mathbf{Q}_1\boldsymbol{\sigma}_0 + \left(\boldsymbol{\sigma}_0{}^T\mathbf{P}_1\right)\left(\mathbf{f}(\mathbf{x}_0,\mathbf{u}) - \mathbf{f}(\hat{\mathbf{x}}_0,\mathbf{u}) + \mathbf{E}\psi(\mathbf{x}_0,\mathbf{u})\right) - \boldsymbol{\sigma}_0{}^T\mathbf{P}_1\mathbf{ESM}^{-1}\dot{\boldsymbol{\xi}}_0 \\ + K_n\boldsymbol{\sigma}_0{}^T\mathbf{P}_1\mathbf{EC}\boldsymbol{\sigma}_0\mathbf{SM}^{-1}\mathbf{N} + \boldsymbol{\sigma}_0{}^T\mathbf{P}_1\mathbf{ESM}^{-1}\mathbf{N}N_\varepsilon(\cdot) - RK_n\boldsymbol{\sigma}_0{}^T\mathbf{P}_1\mathbf{EC}\boldsymbol{\sigma}_0 - R\boldsymbol{\sigma}_0{}^T\mathbf{P}_1\mathbf{E}N_\varepsilon(\cdot). \tag{34}$$

Using (5), (34) becomes

$$\dot{V}_2 = -\boldsymbol{\sigma}_0{}^T\mathbf{Q}_1\boldsymbol{\sigma}_0 + \left(\boldsymbol{\sigma}_0{}^T\mathbf{P}_1\right)\left(\mathbf{f}(\mathbf{x}_0,\mathbf{u}) - \mathbf{f}(\hat{\mathbf{x}}_0,\mathbf{u}) + \mathbf{E}\psi(\mathbf{x}_0,\mathbf{u})\right) - \boldsymbol{\sigma}_0{}^T\mathbf{P}_1\mathbf{ESM}^{-1}\dot{\boldsymbol{\xi}}_0 \\ -(\kappa+R)\boldsymbol{\sigma}_0{}^T\mathbf{P}_1\mathbf{E}N_\varepsilon(\cdot) - (\kappa+R)K_n\boldsymbol{\sigma}_0{}^T\mathbf{P}_1\mathbf{EC}\boldsymbol{\sigma}_0. \tag{35}$$

According to Assumption 5,

$$K_n\boldsymbol{\sigma}_0{}^T\mathbf{P}_1\mathbf{EC}\boldsymbol{\sigma}_0 = K_n\boldsymbol{\sigma}_0{}^T\mathbf{C}^T\mathbf{C}\boldsymbol{\sigma}_0 + K_n\boldsymbol{\sigma}_0{}^T\mathbf{WP}_1\mathbf{EC}\boldsymbol{\sigma}_0, \tag{36}$$

where matrix $\mathbf{W}$ is defined in Assumption 5. Using (36) and Appendix B, (35) can be written as

$$\dot{V}_2 \le -\lambda_{\min}(\mathbf{Q}_1)\|\boldsymbol{\sigma}_0\|^2 + \gamma\|\mathbf{P}_1\|\|\boldsymbol{\sigma}_0\|^2 + \bar{\psi}\|\mathbf{E}\|\|\mathbf{P}_1\|\|\boldsymbol{\sigma}_0\| + \chi_2\|\boldsymbol{\sigma}_0\|\|\mathbf{P}_1\mathbf{ESM}^{-1}\| + (\kappa+R)\|N_\varepsilon(\cdot)\|\|\boldsymbol{\sigma}_0\|\|\mathbf{P}_1\mathbf{E}\| \\ - K_n(\kappa+R)\|\mathbf{C}\boldsymbol{\sigma}_0\|^2 + (\kappa+R)\|\mathbf{WP}_1\|\|\boldsymbol{\sigma}_0\|\left(\mu_0 + \mu_1\|\boldsymbol{\sigma}_0\|\right), \tag{37}$$

where χ_2 is defined in (8), and μ_0 and μ_1 are positive constants defined in Appendix B.

Using Assumption 6 and Young's inequality, it yields

$$\|\boldsymbol{\sigma}_0\|\left[(\kappa+R)\|N_\varepsilon(\cdot)\|\|\mathbf{P}_1\mathbf{E}\| + \bar{\psi}\|\mathbf{P}_1\|\|\mathbf{E}\| + \chi_2\|\mathbf{P}_1\mathbf{ESM}^{-1}\| + \|\mathbf{WP}_1\|(\kappa+R)\mu_0\right] \\ \le \lambda_{\max}(\mathbf{P}_1)\left[\beta_1\|\mathbf{E}\|\|\boldsymbol{\sigma}_0\|^2 + \|\boldsymbol{\sigma}_0\|\left(\beta_2\|\mathbf{E}\| + \bar{\psi}\|\mathbf{E}\| + \chi_2\|\mathbf{ESM}^{-1}\| + \|\mathbf{W}\|(\kappa+R)\mu_0\right)\right] \\ \le \lambda_{\max}(\mathbf{P}_1)\left[\|\boldsymbol{\sigma}_0\|^2\left(\frac{1}{2} + \beta_1\|\mathbf{E}\|\right) + \frac{1}{2}\left(\beta_2\|\mathbf{E}\| + \bar{\psi}\|\mathbf{E}\| + \chi_2\|\mathbf{ESM}^{-1}\| + \|\mathbf{W}\|(\kappa+R)\mu_0\right)^2\right]. \tag{38}$$

Using (38), (37) becomes

$$\dot{V}_2 \le -\lambda_{\min}(\mathbf{Q}_1)\|\boldsymbol{\sigma}_0\|^2 + c_0\|\boldsymbol{\sigma}_0\|^2 - K_n(\kappa+R)\|\mathbf{C}\boldsymbol{\sigma}_0\|^2 + c_1, \tag{39}$$

where

$$c_0 = \gamma\|\mathbf{P}_1\| + \lambda_{\max}(\mathbf{P}_1)\left(\frac{1}{2} + \beta_1\|\mathbf{E}\|\right) + \|\mathbf{WP}_1\|(\kappa+R)\mu_1, \tag{40}$$

and

$$c_1 = \frac{1}{2}\lambda_{\max}(\mathbf{P}_1)\left(\beta_2\|\mathbf{E}\| + \bar{\psi}\|\mathbf{E}\| + \chi_2\|\mathbf{ESM}^{-1}\| + \|\mathbf{W}\|(\kappa+R)\mu_0\right)^2. \tag{41}$$

Now, according to (39), the condition for $\dot{V}_2 \le 0$ is

$$c_0\|\boldsymbol{\sigma}_0\|^2 + c_1 \le K_n(\kappa+R)\|\mathbf{C}\boldsymbol{\sigma}_0\|^2 \\ \le K_n c_2(\kappa+R)\|\mathbf{C}\|^2\|\boldsymbol{\sigma}_0\|^2. \tag{42}$$

where c_2 is a positive constant. This condition can be expressed as

$$\|\boldsymbol{\sigma}_0\|^2 \ge c_1 \Big/ \left(K_n c_2(\kappa+R)\|\mathbf{C}\|^2 - c_0\right). \tag{43}$$

Now, by defining the following compact set around the origin:

$$\Theta := \left\{\boldsymbol{\sigma}_0 \,\middle|\, \|\boldsymbol{\sigma}_0\|^2 \le c_1 \Big/ \left(K_n c_2(\kappa+R)\|\mathbf{C}\|^2 - c_0\right)\right\}, \tag{44}$$

it can be concluded that $\dot{V}_2 \le 0$ when the error is outside the compact set Θ. Hence, according to the extension of the standard Lyapunov theorem (Narendra and Annaswamy, 1995), the error trajectory $\boldsymbol{\sigma}_0$ is ultimately bounded. Moreover, this bound can be made small using large values for K_n. □

Remark 3: According to (44), increasing K_n (i.e. the relay equivalent gain) makes the compact set Θ smaller. I.e., increasing the relay equivalent gain provides smaller tracking errors for the observer. However, as it will be shown in Section 4, increasing K_n has practical limitations and cannot be increased without any bound.

As Theorem 1 shows, in addition to vector $\mathbf{L}$, K_n also affects the dynamics of the slow-mode part in the sliding phase. In the next sections, it will be shown that K_n is a function of the amplitude and frequency of oscillations. Hence, K_n can be controlled by parameters of the fast-mode dynamics of the observer such as $H(s)$ and Ω_s.

3.2.2.2. Fast-mode dynamics of observer in sliding phase

In Theorem 1, it was shown that the slow-mode part of the observer error dynamics can be made very small by appropriate design of the relay equivalent gain in the slow-mode part (i.e. K_n). In the followings, the fast-mode part of the observer in the sliding phase is analyzed. First, consider the fast-mode dynamics of the observer presented in (32).

Assumption 7: Based on the fast-mode part of the observer, given in (32), matrices $\mathbf{L}$ and $\mathbf{E}$ and scalar K_s can be defined such that the following matrix has negative eigenvalues:

$$\mathbf{A}_s = \begin{bmatrix} \bar{\mathbf{A}} - K_s R\mathbf{EC} & -\mathbf{ES} \\ K_s\mathbf{NC} & \mathbf{M} \end{bmatrix}. \tag{45}$$

Hence, stability of the fast-mode part of the observer is guaranteed by stable eigenvalues of $\mathbf{A}_s$.

According to (32), the fast-mode part of the observer in the sliding phase can be decomposed into the cascade connection of the following linear systems:

$$\mathrm{G}_\mathrm{f}: \begin{cases} \dot{\boldsymbol{\sigma}}_s = (\mathbf{A} - \mathbf{LC})\boldsymbol{\sigma}_s + \mathbf{E}(-\bar{y}_s) \\ e_s = \mathbf{C}\boldsymbol{\sigma}_s \end{cases} \tag{46}$$

$$H: \begin{cases} \dot{\boldsymbol{\xi}}_s = \mathbf{M}\boldsymbol{\xi}_s + \mathbf{N}(K_s e_s) \\ \bar{y}_s = \mathbf{S}\boldsymbol{\xi}_s + R(K_s e_s) \end{cases} \tag{47}$$

where e_s is the output of $G_\mathrm{f}(s)$ and $K_s e_s$ is the fast-mode part of the input to $H(s)$. According to Definition 1 and Remark 1, $y_s(t) = 0$; then, $e_s(t) = y_s(t) - \hat{y}_s(t) = -\hat{y}_s(t)$. Figure 2 shows the structure of the fast-mode part of the observer.

According to (46) and (47), the relation between the input and output of the relay element for the fast-mode part in the frequency domain is equal to the inverse of the transfer function of the relay element in the fast-mode operation

$$|K_s| = \frac{1}{|G_\mathrm{f}(j\Omega_s)||H(j\Omega_s)|}. \tag{48}$$

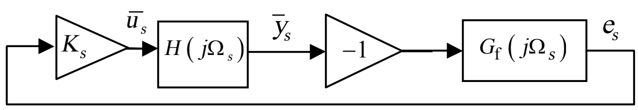

Figure 2. Fast-mode dynamics of observer.

On the other hand, using (25), (26) and (48), it gives

$$|K_n| = \frac{1}{2|G_f(j\Omega_s)||H(j\Omega_s)|}. \tag{49}$$

As it was shown in this section, the relay equivalent gain for the fast- and slow-mode parts can be regulated by appropriate design of the linear systems $G_f(s)$ and $H(s)$, and the frequency of oscillations Ω_s. In other words, the larger $|G_f(j\Omega_s)||H(j\Omega_s)|$ the smaller K_n and K_s. Based on Theorem 1, these parameters directly affect the stability and the estimation error of the observer.

Equations (46), (47) and (49) help the designer to determine an appropriate value for K_n. The frequency and amplitude of oscillations will be considered in the followings.

According to the theory of self-oscillating adaptive systems (based on the relay feedback systems), $H(s)$ can be designed such that the frequency of oscillations (or the limit cycle) Ω_s, with the following property (Åström and Wittenmark, 1995):

$$\angle G_f(j\Omega_s) + \angle H(j\Omega_s) = -180^0, \tag{50}$$

can be controlled as desired. Moreover, the amplitude of oscillations for the fast-mode part can be derived using (25) and (49) as

$$a = \frac{4d}{\pi}|G_f(j\Omega_s)||H(j\Omega_s)|. \tag{51}$$

Since the amplitude of $|G_f(j\Omega)|$ is a decreasing function with respect to the frequency, larger selections of Ω_s lead to smaller values of $|G_f(j\Omega)|$ and consequently, larger values for K_n and K_s. Therefore, making the switching frequency large enough and far enough from the bandwidth of the slow-mode part of the observer has two benefits: 1) The oscillating mode of signals can be easily removed using a low-pass filter and 2) According to Theorem 1 and (49), the relay equivalent gain becomes large in the sliding phase. Hence, the observer acts as a high-gain observers, which provides faster transient times and better disturbance rejections. This property moves the observer closer to the ideal sliding-mode condition, where the switching frequency grows to infinite. The following theorem shows conditions for the ideal sliding mode.

Theorem 2. If the transfer function $W_l(s)$ is a quotient of two polynomials $B_m(s)$ and $A_n(s)$ with degrees m and n, respectively, with non-negative coefficients, then for the existence of the ideal sliding mode it is necessary that the relative degree (n–m) of $W_l(s)$ be one or two.

Proof: See (Boiko, 2008).

Remark 4: According to Theorem 2, when condition (50) is not satisfied (i.e. when the relative degree of $G_f(s)H(s)$ is less than two, and for some systems equal to two), then the ideal sliding mode occurs. In other words, the deal sliding mode condition occurs when there is no $\Omega \geq 0$ that satisfies (50).

In the ideal sliding-mode condition, the switching frequency grows without any bound. However, in practice, since the sampling time τ is not zero, the switching frequency cannot be infinite. In this condition, the oscillation frequency obeys the following equation (Boiko and Fridman, 2006; Boiko, 2008):

$$\angle G_{\mathrm{f}}\left(j\Omega_{s}\right)+\angle H\left(j\Omega_{s}\right)+\angle \exp(-j\Omega_{s}.\tau)=-180^{0}\,. \tag{52}$$

Therefore, it can be concluded that for systems that $G_{\mathrm{f}}(s)\,H(s)$ satisfies the ideal sliding-mode condition, the switching frequency grows to the largest possible switching frequency that it can be computed from (52).

Remark 5: According to the fast-mode dynamics of the observer (G_{FM}), presented in (46) and (47), **E**, $H(s)$ and **L** should be such that conditions given in Theorem 2 (i.e. conditions for the ideal sliding mode) are satisfied. Hence, as it was mentioned before, the relative degree of $H(s)$ should be zero.

4. Uncertainty effect reduction and *H*(*s*) design

In the last section, it was showed that the relay equivalent gain can be controlled by proper design of $G_{\mathrm{f}}(s)$ and $H(s)$. Moreover, it was showed that the higher the relay equivalent gain, the smaller the estimation error.

In this section, first, the relationship between the sampling time and the relay equivalent gain will be analyzed. Then, a procedure for the design of *H*(*s*) will be given. Generally, the observer can be made robust with respect to the uncertainties and disturbances by increasing the relay gain *d*. This means that for larger disturbances and uncertainties there is need for larger values for *d* in order to keep the observer in the sliding phase. However, according to (51), larger values for *d* make the amplitude of oscillations larger. Nevertheless, larger amplitude of oscillations does not have any effect on the estimation error, according to Theorem 1. In other words, the estimated signals of the slow-mode part is affected by the relay equivalent gain K_{n} and not *d*. That is, larger K_{n} will reduce the estimation errors in the presence of larger uncertainties.

Although the ideal sliding-mode condition provides large relay equivalent gains, but in some cases this gain is not enough for damping the effects of uncertainties for the state estimation.

The next two subsections will demonstrate ways of increasing the relay equivalent gain to improve the quality of state estimations in the presence of uncertainties.

4.1. High relay equivalent gain by reduction of sampling time

In this section, it will be shown that smaller sampling time (τ) provides larger relay equivalent gain to the observer. First, it is assumed that $H(s)=1$ (i.e no linear compensator exists). Let $G_{\mathrm{f}}\left(j\Omega\right)$ be a first order system and then in the switching frequency, which is large enough, the phase condition is $\angle G_{\mathrm{f}}\left(j\Omega_{s}\right)+\angle H\left(j\Omega_{s}\right)=-90^{0}$. This condition, according to Remark 4, shows that the ideal sliding-mode condition is satisfied. According to (52) and for a certain sampling time (τ), the switching frequency (Ω_{s}) grows until the following condition is satisfied:

$$\angle \exp(-j\Omega_{s}\tau)=-90^{0}\,. \tag{53}$$

Therefore, $\Omega_{s}\tau=\text{constant}$. In other words, decreasing the sampling time yields larger switching frequencies and vice versa. Consequently, $\left|G_{\mathrm{f}}\left(j\Omega\right)\right|$ will be smaller for smaller sampling times since $\left|G_{\mathrm{f}}\left(j\Omega\right)\right|$ is a decreasing function of the frequency. As a result, according to (49), the relay equivalent gain (K_{n}) becomes larger. Thus, decreasing the sampling time in sliding-mode observers makes the relay equivalent gain larger. According to Theorem 1 and Remark 3, larger relay equivalent gains provide better state estimation or less estimation errors in the slow mode.

In practice, smaller sampling time requires hardware improvements. In the next section, a method will be proposed that can provide larger relay equivalent gains without any need for smaller sampling time.

4.2. Providing high equivalent gain of relay by Design of *H*(*s*)

In this section, it is shown that the relay equivalent gain can be increased using the compensator *H*(*s*), without any need for decreasing the sampling time. This goal is achieved by proper frequency domain design of *H*(*s*) based on (49) and (52). The main idea is based on (49), where increasing K_n can be achieved by decreasing $\left|H\left(j\Omega_s\right)\right|$. Hence, $H(s)$ must have the following properties:

1. In the low frequency domain, $H(s)$ must have considerable amplitude in order to make the observer fast enough and pass the low-frequency signals. For instance, it can be equal to one.
2. In the switching frequency, $\left|H\left(j\Omega_s\right)\right|$ must be decreased in order to obtain larger values for K_n.
3. The ideal sliding mode conditions, mentioned in Theorem 2, must be provided. Hence, based on Remark 5, the relative degree of $H(s)$ should be zero.

By satisfying the above three conditions, the observer will have better transient response when it is close to the sliding surface, the relay equivalent gain will be sufficiently increased, and a limit cycle with higher switching frequencies will be generated, respectively.

Remark 6: Condition 2 is the main part of the design. It should be noted that decreasing $\left|H\left(j\Omega\right)\right|$ around the switching frequency makes the phase of $H\left(j\Omega\right)$ negative. This property, based on (52), reduces the switching frequency and consequently increases $\left|G_f\left(j\Omega_s\right)\right|$, which in turn neutralizes the reduction of $\left|H\left(j\Omega_s\right)\right|$. In order to avoid this undesired phenomenon, $\left|H\left(j\Omega_s\right)\right|$ should be decreased before the switching frequency with enough margins, in order to have less negative phase for $H\left(j\Omega\right)$ in the switching frequency.

Remark 7: Based on Remark 6, decreasing $\left|H\left(j\Omega\right)\right|$ in the low frequencies may violate Condition 1. That is, the bandwidth of the observer would be decreased yielding bad transient responses for the state estimation. In order to avoidance this unwanted phenomenon, d is increased for $0 \le t \le t_s$, where t_s is the instance when the sliding-mode occurs. Hence, larger amplitude for d for $0 \le t \le t_s$ compensates reduction in the observer bandwidth. Then, after the sliding-mode occurs, d will be decreases to the original value determined based on Lemma 1.

Although in the proposed observer, the relay equivalent gain grows to a larger value than the ideal sliding mode observer, but as it was discussed in Remarks 6 and 7, this property has some limitations that are due to the restrictions of frequency domain design of $H(s)$.

5. Application to a bioreactor

In this section, the performance of the proposed observer is illustrated by applying it to a bioreactor with biomass production and substrate concentration that belongs to the class of (1). The nonlinear state equations of this system are (Gauthier et al., 1992; Bernard et al., 1998)

$$\dot{x}_1(t)=\frac{\mu_m x_1(t)x_2(t)}{K_m x_1(t)+x_2(t)}-Dx_1(t)$$
$$\dot{x}_2(t)=-\frac{1}{Y}\frac{\mu_m x_1(t)x_2(t)}{K_m x_1(t)+x_2(t)}+\left(s_f-x_2(t)\right)D, \tag{54}$$

where the specific growth rate is assumed to follow the Contois model, x_1 is the biomass concentration, x_2 is the substrate concentration, s_f is the inlet substrate concentration, D is the dilution rate, K_m is the reaction constant, Y is the yield of cell mass and μ_m is the maximal specific growth rate. It is assumed that the biomass $x_1(t)$ is measurable on-line by a biosensor (Ducommun et al., 2002). Farza et al. have shown that this system is observable (2009). In practice, μ_m and K_m may be uncertain and time-varying. Hence, let consider $\mu_m=\mu_m^0+d_1(t)$ and $K_m=K_m^0+d_2(t)$, where μ_m^0 and K_m^0 are the known nominal parameters, and $d_1(t)$ and $d_2(t)$ model the bounded additive time-varying parametric uncertainties. Therefore, based on (1), the uncertain system is defined as

$$\dot{x}_1(t)=\frac{\mu_m^0 x_1(t)x_2(t)}{K_m^0 x_1(t)+x_2(t)}-Dx_1(t)+\psi(\mathbf{x},t),$$
$$\dot{x}_2(t)=-\frac{1}{Y}\frac{\mu_m^0 x_1(t)x_2(t)}{K_m^0 x_1(t)+x_2(t)}+\left(s_f-x_2(t)\right)D-\frac{1}{Y}\psi(\mathbf{x},t) \tag{55}$$

where $\psi(\mathbf{x},t)=\frac{\mu_m x_1(t)x_2(t)}{K_m x_1(t)+x_2(t)}-\frac{\mu_m^0 x_1(t)x_2(t)}{K_m^0 x_1(t)+x_2(t)}$ is an unknown function.

In addition, the model and observer simulations have been carried out using a constant input substrate concentration and dilution rate. The parameter values used in simulations are

$$\mu_m^0=1\,\mathrm{h}^{-1},\ K_m^0=1,\ Y=1,\ D=0.5\,\mathrm{h}^{-1},\ s_f=5\ \mathrm{g.l}^{-1},\ d_1=1\sin(1.5\pi t),\ d_2=0.9\sin\left(\pi t-\pi/4\right).$$

The goal is to design a sliding-mode observer based on (3) and (4) to estimate the process states in presence of model uncertainty using the method developed in this paper.

Using the pole placement technique, the feedback gain is $\mathbf{L}=[2\ \ -1]^T$. This gain satisfies condition (12) with

$$\mathbf{P}_1=\begin{bmatrix}0.5556 & -0.444\\ -0.444 & 0.5556\end{bmatrix}. \tag{56}$$

Then, according to Assumption 5, it gives

$$\mathbf{W}=\begin{bmatrix}0 & 0\\ 0 & 1\end{bmatrix},\ \bar{\mathbf{C}}=\begin{bmatrix}0 & -1\end{bmatrix}^T. \tag{57}$$

Based on Lemma 1, the amplitude of the relay gain is selected as $d=50$.

According to (46), for $\mathbf{E}=[1\ \ -1]^T$, it gives

$$G_f(s)=1/(s+2.5), \tag{58}$$

which is a stable system with the relative degree of one. The initial states of the system and the observer are selected as $\mathbf{x}(0)=[2\ \ 2]^T$ and $\hat{\mathbf{x}}(0)=[1\ \ 1.5]^T$, respectively.

Figure 3 shows the tracking error for the state variable x_1 for different values of the relay gain d, fixed sampling time and $H(s)=1$. As this figure shows, changing the value of d just changes the amplitude of oscillations and does not have any effect on the estimation quality. Next, the effect of the sampling time on the state estimation in the presence of uncertainty is analyzed. Simulations are carried out for three cases: $\tau=0.001$ s, $\tau=0.0005$ s, and $\tau=0.0001$ s. Figure 4 shows the tracking error for the state variable x_1. Using (52), the period of oscillations for three sampling times are equal to $T = 4\times10^{-3}$ s, $T = 2\times10^{-3}$ s, and $T = 4\times10^{-4}$ s, respectively. These values can also be observed from Figure 4. As it was discussed in Section 4.1, and as Figure 4 shows, smaller sampling times provide better state estimation.

Next, the proposed method is applied to the bioreactor system. Based on three conditions given in Section 4.2, $H(s)$ is designed as

$$H(s) = (0.011s + 1)/(0.32s + 1)\,. \tag{59}$$

Figure 5 shows the bode diagram of $H(s)$.

By selecting the sampling time equal to $\tau = 1\times10^{-3}$ s and solving (52), the switching frequency and the period of oscillations for e will be equal to $\Omega_s \approx 1495$ rad/s and $2\pi/\Omega_s = 4.2\times10^{-3}$ s, respectively. Figure 5 shows that Conditions 1 and 2 are satisfied in the design procedure. In addition, since the relative degree of $G_f(s)H(s)$ is one, Condition 3 (the ideal sliding-mode condition) is also satisfied. Now, according to (49), the relay equivalent gain for the slow-mode part of the proposed observer becomes

$$K_n = \frac{1}{2|G_f(j\Omega_s)||H(j\Omega_s)|} = \frac{1}{2\times(0.000668\times0.0343)\times1} = 21826\,. \tag{60}$$

Based on (51), the amplitude of oscillations of e (the input to the relay element) is

$$a = \frac{4d}{\pi}|G_f(j\Omega_s)||H(j\Omega_s)| = \frac{4\times50\times0.000668\times0.0343}{\pi} = 0.0015\,. \tag{61}$$

In addition, according to (45), all the eigenvalues of $\mathbf{A}_s$ are real and negative, which guarantees stability of the fast-mode dynamics of the observer.

According to Remark 7, in order to have better reaching phase, d=2000 for $0 \le t \le t_s$ and d= 50 for $t > t_s$. Figure 6 shows the output tracking error e. As this Figure indicates, the period and amplitude of oscillations for e are equal to 4.2×10^{-4} s and 16.5×10^{-4}, respectively. These numbers agree with the values obtained using equations (52) and (51), respectively. It should be noted that for the conventional SMO, the observer parameters are $K_n = 748$ and $a = 0.043$. Figure 7 shows the estimated states of the plant using the proposed observer. In order to present an illustrative comparison between the proposed observer and the convention SMO, estimation errors are presented in Figure 8. In addition, Table 1 presents integral of the estimation errors during the steady state ($t \ge 15s$) for a) the proposed observer with $\tau = 0.001$ s, b) the conventional SMO with $\tau = 0.001$ s, and c) the conventional SMO with $\tau = 0.0001$ s. As Figure 8 and Table 1 show, the proposed observer provides less estimation error and is less affected by the uncertainty as compared to the conventional SMO even with smaller sampling time. Moreover, the proposed observer reduces the amplitude of oscillations. As a result, it can be concluded that the proposed observer improves the conventional SMO in presence of large uncertainties. Moreover, the proposed observer can reduce the effect of the measurement noise in the state estimation as compared to the convention SMO. This property is due to the low pass filtering property of $H(s)$. Figure (9) shows this property of the proposed observer for σ_2 in the presence of white noise with uniform distribution in [–0.1, 0.1].

σ_1

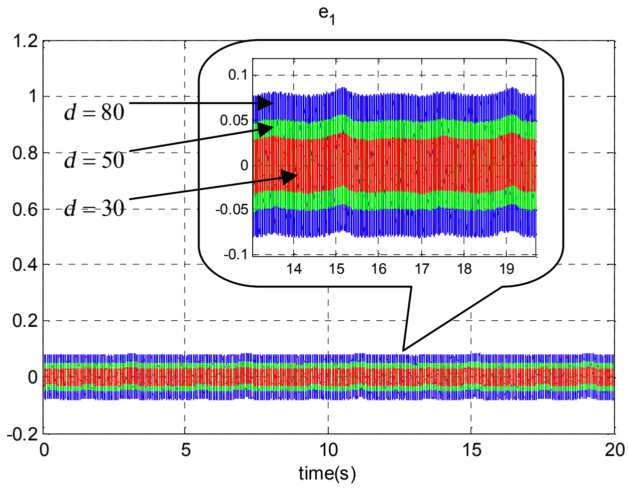

Figure 3. Tracking error (σ_1) using conventional SMO with different values for d

σ_1

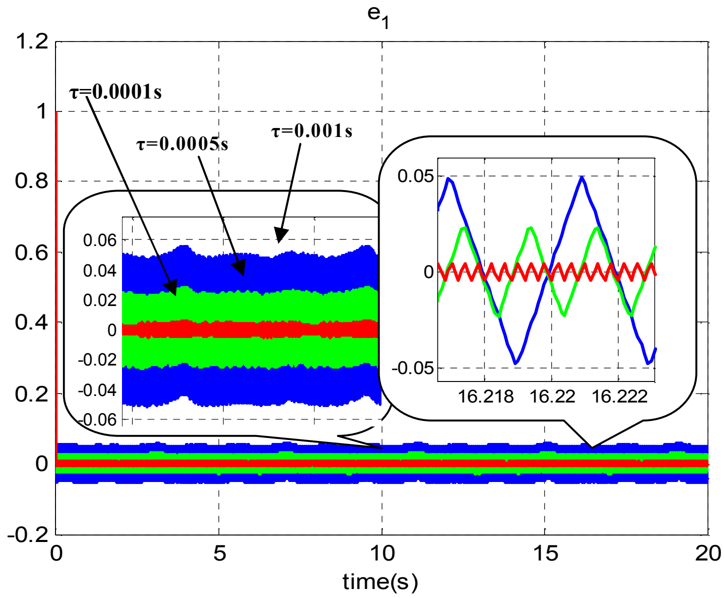

Figure 4. The tracking error (σ_1) using conventional SMO with different sampling times and fixed d

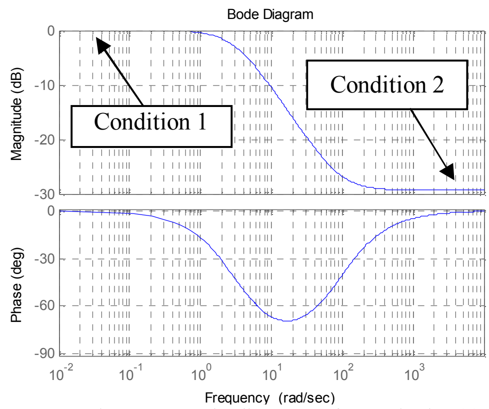

Figure 5: Bode diagram of a typical $H(s)$

σ_1

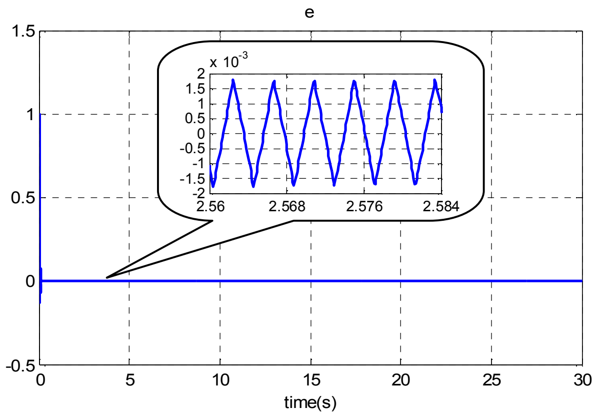

Figure 6. Input signal of the relay element (σ_1) for the proposed method

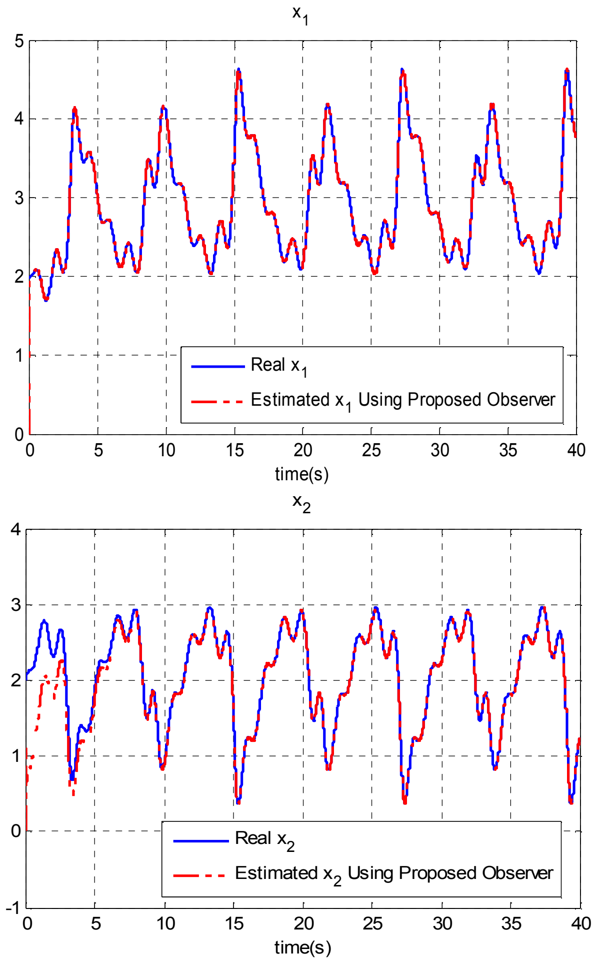

Figure 7. Estimation of states using the proposed observer

Table 1: Summary of tracking errors in the steady state stage for conventional SMO and proposed method

	SMO with $\tau = 0.001$	SMO with $\tau = 0.0005$	Proposed Observer with $\tau = 0.001$
$\int_{t=15}^{t=40} \sigma_1(t)dt$	10.77	5.92	0.32
$\int_{t=15}^{t=40} \sigma_2(t)dt$	-29.02	-14.24	0.61

σ_1

σ_2

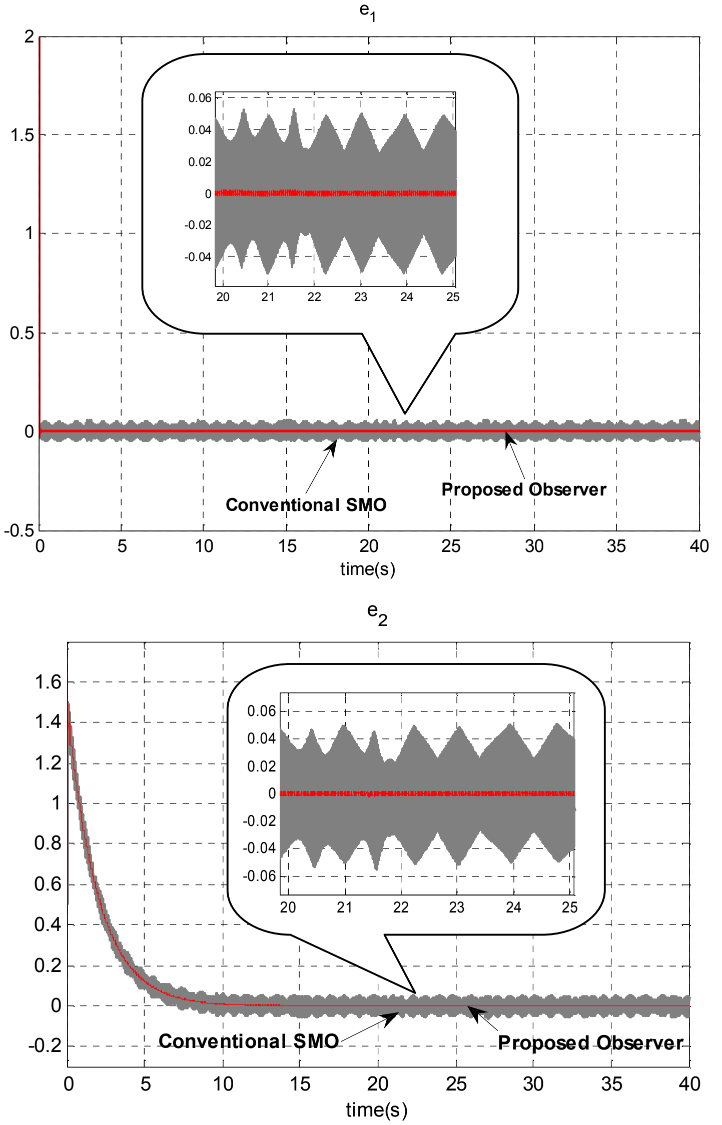

Figure 8. Estimation errors using conventional SMO and proposed observer with $\tau = 0.001$.

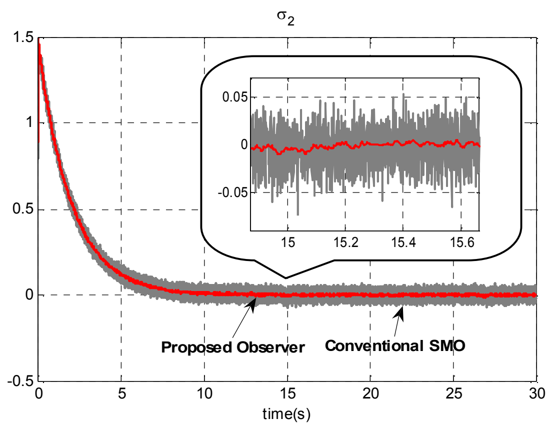

Figure 9. Estimation errors in presence of measurement noise

6. CONCLUSION

Designing a relay based sliding-mode observer was introduced in this paper. This observer uses the high gain property before the sliding phase occurs in order to have fast response and also providing conditions for reaching the sliding surface. Then, in the sliding phase, signals are decomposed into the slow- and fast-mode parts. One of the main contributions of this paper is that it provides a method for analysis of the fast- and slow-mode parts of signals in the sliding phase in nonlinear sliding-mode observers. Moreover, it shows the relation between these modes. In addition, relation between the sampling time and accuracy in SMO is analyzed. It was shown that the relay equivalent gain increases by decreasing the sampling time. Additionally, by introducing a new approach, an appropriate linear compensator was cascaded with the SMO such that the high-gain observer properties are provided for the slow-mode dynamics of the observer. This method has two benefits: 1) it improves the ability of better state estimation in the presence of large uncertainties without any need for reducing the sampling time and 2) reduction of the amplitude of oscillations in SMO. Simulation results on a bioreactor process show that the proposed technique provides good tracking in the presence of large uncertainties as compared to the conventional SMO that uses even smaller sampling times.

References

Aguilar-López, R., Martínez-Guerra, R. & Maya-Yescas, R. (2003) State estimation for partially unknown nonlinear systems: a class of integral high gain observers. *IEE Proceedings Control Theory & Applications*, **150**, 240- 244.

Ahrens, J. H. & Khalil, H. K. (2009) High-gain observers in the presence of measurement noise: A switched-gain approach. *Automatica*, **45**, 936-943.

Åström, K. J. & Wittenmark, B. (1995) *Adaptive Control*, Reading, MA: Addison-Wesley.

Atherton, D. P. (1975) *Nonlinear Control Engineering: Describing Function Analysis and Design*. London: Van Nostrand Reinhold, 1975.

Bernard, O., Sallet G. & Sciandra, A. (1998) Nonlinear observers for a class of biological systems: application to validation of a phytoplanktonic growth model. *IEEE Transactions on Automatic Control*, **43**, 1056–1065.

Boiko, I. (2005) Analysis of sliding modes in the frequency domain. *International Journal of Control*, **78**, 969–981.

Boiko, I. (2007) Analysis of closed-loop performance and frequency-domain design of compensating filters for sliding mode control systems. *IEEE Transactions on Automatic Control*, **52**, 1882-1891.

Boiko, I. (2008) *Discontinuous Control Systems: Frequency-Domain Analysis and Design*, Boston: Birkhäuser.

Boiko, I. (2009) Frequency domain analysis of accuracy of sliding mode observers under imperfect knowledge of model parameters, *IEEE Transactions on Automatic Control*, **54**, 2446-2450.

Boiko, I. & Fridman, L. (2006) Frequency domain input–output analysis of sliding-mode observers. *IEEE Transactions on Automatic Control*, **51**, 1798-1803.

Boiko, I., Fridman, L., Pisano, A. & Usai, E. (2009) On the transfer properties of the generalized sub-optimal second-order sliding mode control algorithm. *IEEE Transactions on Automatic Control*, **54**, 399-403.

Cunha, J. P., Costa, R. R., Lizarralde, F. & Hsu, L. (2009) Peaking free variable structure control of uncertain linear systems based on a high-gain observer. *Automatica*, **45**, 1156-1164.

Ducommun, P., Kadouri, A., von Stockar, U. & Marison, I. W. (2002) Online determination of animal cell concentration in two industrial high density culture processes by dielectric spectroscopy. *Biotechnology and Bioengineering*, **77,** 316- 322.

Farza, M., M'Saada, M., Maatouga, T. & Kamounb, M. (2009) Adaptive observers for nonlinearly parameterized class of nonlinear systems, *Automatica*, **45**, 2292-2299.

Floquet, T., Edwards, C. & Spurgeon, S. K. (2007) On sliding mode observers for systems with unknown inputs. *International Journal of Adaptive Control and Signal Processing*, **21**, 638-656.

Gauthier, J. P., Hammouri, H. & Othman, S. (1992) A simple observer for nonlinear systems applications to bioreactors, *IEEE Transactions on Automatic Control*, **37**, 875–880.

Hajatipour, M., Farrokhi, M. (2010) Chattering free with noise reduction in sliding-mode observers using frequency domain analysis, *Journal of Process Control*, **20**, 912-921.

Haskara, I., Özgüner, U. & Utkin, V. (1998) On sliding mode observers via equivalent control approach. *International Journal of Control*, **71**, 1051-1067.

Kailath, T. (1980) *Linear Systems*, New Jercy: Prentice-Hall.

Khalil, H. K. (1996) *Nonlinnear Systems*, New Jercy: Prentice-Hall.

Koshkouei, A. J. & Zinober, S.I. (2004) Sliding mode state observation for non-linear systems, *International Journal of Control*, **77**, 118-127.

López, R. A. & Yescas, R. M. (2005) State estimation for nonlinear systems under model uncertainties: a class of sliding-mode observers. *Journal of Process Control*, **15**, 363–370.

Narendra, K. S. & Annaswamy, A. M. (1995) *Stable Adaptive System*, London: Prentice-Hall.

Pan, Y., Kumar, K. D., Liu, G. & Furuta, K. (2009) Design of variable structure control system with nonlinear time-varying sliding sector. *IEEE Transactions on Automatic Control*, **54**, 1981-1986.

Picó, J., Battista, H. D. & Garelli, F. (2009) Smooth sliding-mode observers for specific growth rate and substrate from biomass measurement. *Journal of Process Control*, **19**, 1314–1323.

Slotine, J. E. & Li, W. (1991) *Applied Nonlinear Control*, New Jercy: Prentice-Hall.

Spurgeon, S. K. (2008) Sliding mode observers: a survey. *International Journal of Systems Science*, **39**, 751–764.

Tsypkin, Y. Z. (1984) *Relay Control Systems*. Cambridge: Cambridge University Press.

Utkin, V. (1992) *Sliding Modes in Control and Optimization*, Berlin: Springer-Verlag.

Vasiljevic, L. K. & Khalil, K. (2008) Error bounds in differentiation of noisy signals by high-gain observers. *Systems & Control Letters*, **57**, 856–862.

Veluvolu, K. C., Soh, Y.C. & Cao, W. (2007) Robust observer with sliding mode estimation for nonlinear uncertain systems. *IET Control Theory and Applications*, **1**, 1533–1540.

Zheng, Y., Abdel Fattah, H. A. & Loparo, K. A. (2000) Non-linear adaptive sliding mode observer controller scheme for induction motors. *International Journal of Adaptive Control and Signal Processing*, **14**, 245-273.

Appendix A

From the theory of linear systems (Kailath, 1980), the output of $H(s)$ for $0 \le t \le t_s$, where t_s denotes the instant that the sliding phase occurs, is determined as follow:

$$\bar{y}(t) = \mathbf{S}e^{\mathbf{M}t}\xi(t_0) + \mathbf{S}\int_0^t e^{\mathbf{M}(t-\tau)}\mathbf{N}\bar{u}(\tau)\,d\tau + R\bar{u}(t)\,.$$

Since $\bar{u}(\tau) \in \{1, -1\}$ and is fixed before the sliding phase occurs then,

$$\begin{aligned}\bar{y}(t) &= \mathbf{S}e^{\mathbf{M}t}\xi(t_0) + \mathbf{SM}^{-1}e^{\mathbf{M}t}\left(\mathbf{I} - e^{\mathbf{M}(-\tau)}\right)\mathbf{N}\bar{u}(t) + R\bar{u}(t) \\ &= \mathbf{S}e^{\mathbf{M}t}\xi(t_0) + \left(\mathbf{SM}^{-1}e^{\mathbf{M}t}\mathbf{N} - \mathbf{SM}^{-1}\mathbf{N} + R\right)\bar{u}(t)\end{aligned}$$

Appendix B

Using (31), the slow-mode part of the observer in the sliding phase is

$$\dot{\boldsymbol{\sigma}}_0 = \bar{\mathbf{A}}\boldsymbol{\sigma}_0 - \mathbf{ES}\xi_0 + \left(\mathbf{f}(\mathbf{x},\mathbf{u}) - \mathbf{f}(\hat{\mathbf{x}},\mathbf{u})\right) + \mathbf{E}\psi(\mathbf{x}_0,\mathbf{u}) - RN_\varepsilon(\cdot)\mathbf{E} - RK_n\mathbf{EC}\boldsymbol{\sigma}_0\,.$$

Since in the sliding phase $\left\|\dot{\boldsymbol{\sigma}}_0(t)\right\| \le \chi_3$, where χ_3 is defined as the upper bound, then from the last equation it can be concluded that

$$\left\|K_n\mathbf{EC}\boldsymbol{\sigma}_0\right\| \le \mu_0 + \mu_1\left\|\boldsymbol{\sigma}_0\right\|$$

where

$$\mu_0 = \left(1/R\right)\left[\chi_3 + \|R\mathbf{E}\|\beta_2 + \|\mathbf{ES}\|\chi_1 + \|\mathbf{E}\|\overline{\psi}\right]$$

and

$$\mu_1 = \left(1/R\right)\left[\|\overline{\mathbf{A}}\| + \gamma + \|R\mathbf{E}\|\beta_1\right].$$

Hence,

$$\begin{aligned}\left\|K_n \boldsymbol{\sigma}_0{}^T \mathbf{W}\mathbf{P}_1 \mathbf{E}\mathbf{C}\boldsymbol{\sigma}_0\right\| &\le \left\|\boldsymbol{\sigma}_0{}^T \mathbf{W}\mathbf{P}_1\right\| \left\|K_n \mathbf{E}\mathbf{C}\boldsymbol{\sigma}_0\right\| \\ &\le \|\mathbf{W}\mathbf{P}_1\| \|\boldsymbol{\sigma}_0\| \left(\mu_0 + \mu_1 \|\boldsymbol{\sigma}_0\|\right).\end{aligned}$$